Metallurgy Department. Progress report for the period 1 April 1971 to 31 December 1972

Research Establishment Risø, Roskilde

Publication date:
1973

Document Version
Publisher's PDF, also known as Version of record

Danish Atomic Energy Commission

Research Establishment Risø

Metallurgy Department Progress Report

for the Period 1 April 1971 to 31 December 1972

March 1973

Sales distributors: Jul. Gjellerup, 87, Sølvgade, DK-1307 Copenhagen K, Denmark

Available on exchange from: Library, Danish Atomic Energy Commission, Risø, DK-4000 Roskilde, Denmark

UDC. 669

March 1973

Risø Report No. 274

Danish Atomic Energy Commission

Research Establishment Risø

METALLURGY DEPARTMENT PROGRESS REPORT

for the Period 1 April, 1971 to 31 December, 1972

Fi 25

ISBN 87 550 0175 0

CONTENTS

INTRODUCTION

This report represents a new style of Metallurgy Department annual reports. A general view of the activities in the past year is presented in the introduction. Two selected topics are then given a more detailed treatment, and the participation in international collaboration and the activities within education and training are described in separate chapters. In the survey of publications abstracts have been added. The period covered by the report has been changed to the calender year instead of the Danish financial year, hence this report covers the period 1 April, 1971 to 31 December, 1972. We hope that this new annual report will give a clear and coherent picture of our work.

To supplement the description of activities in the following it should be mentioned that the organization of the department is being changed towards a more project-oriented structure. This should result in more direct participation of the staff members in the decisions concerning the research work, and thereby hopefully contribute positively to the efficiency of the department.

The collaboration with Danish industry on non-nuclear projects is an important part of the activities of the Metallurgy Department. A new way of organizing this collaboration was tried: Individual staff members devote part of their time to develop the contact with specific companies. This arrangement proved beneficial to the department in providing a number of research contracts. It is our impression that the companies involved are also well satisfied with the arrangement. A technical description of the industrial work is outside the scope of this report, and a special publication on the subject of industrial collaboration has been issued (in Danish only).

General Materials Research

This work covered research programmes on the deformation, strength, and structure of single-phase and two-phase materials, fracture mechanics and some fundamental aspects of the behaviour of zirconium alloys.

A method was developed for the determination of dislocation segment length distributions from the projected segment lengths observed by transmission electron.microscopy. The method was applied to creep-deformed magnesium oxide with the aim of correlating the dislocation structure to the creep behaviour.

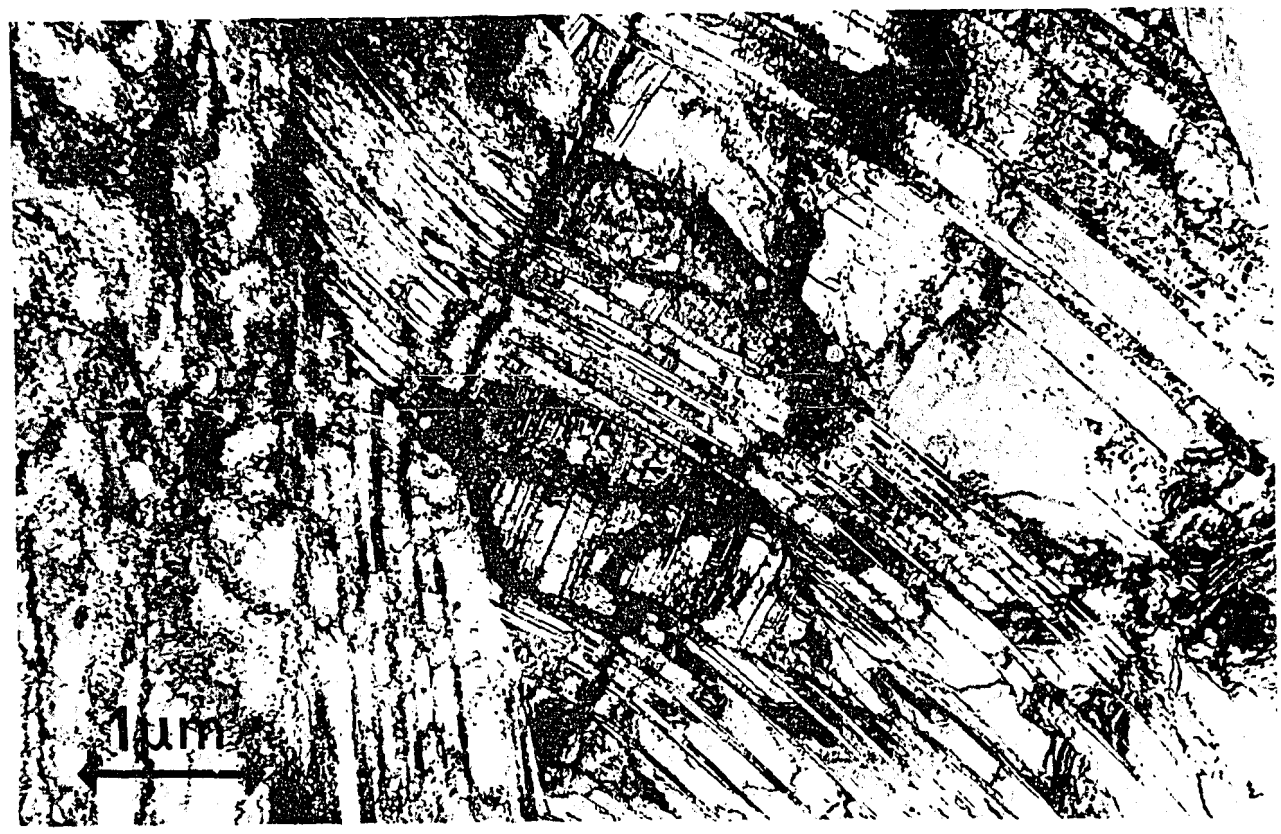

Fig. 1. Brass rolled to 42% reduction. The deformation inhomogeneities are revealed by the bending of the deformation-twin lamellae.

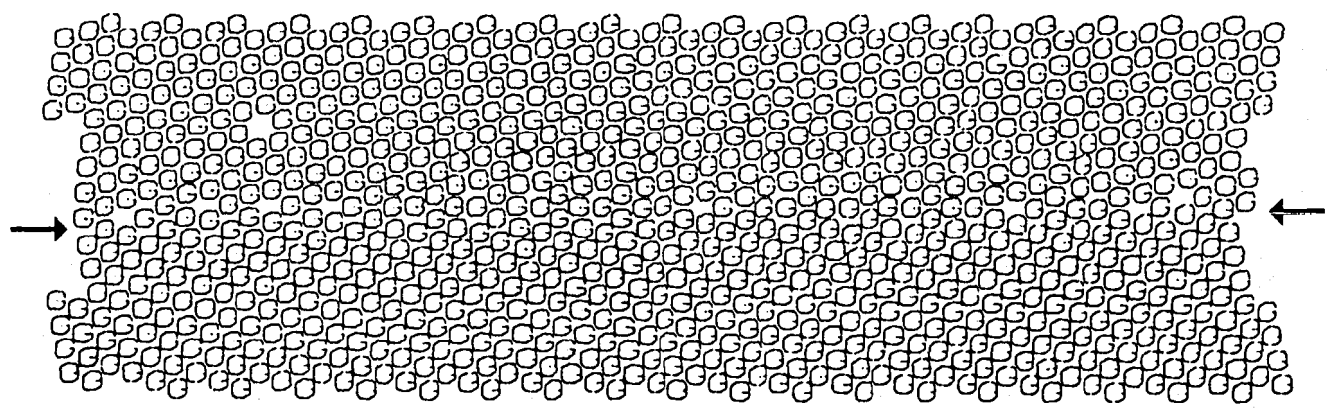

Fig. 2. Computer-generated grain boundary - the approximate position of the boundary is marked with arrows. A vacancy is seen in the lattice above the boundary.

On the basis of the rolling texture a model has been proposed for the plastic deformation of face-centred cubic polycrystals (Risø Report No. 199 (1969) pp. 16-17). An exhaustive electron-microscopical investigation of the microstructure of f.c.c. materials after plastic deformation underlined the importance of the deformation inhomogeneities (see fig. 1). The model was modified accordingly so that the inhomogeneity of the deformation process is given a more active role in the plastic deformation. Apart from making the model agree better with experiment, this change also produced a more logical and coherent model.

The formation of grain boundaries was computer-simulated by molecular dynamics techniques (in collaboration with the Department of Structural Properties of Materials at the Technical University of Denmark). A two-dimensional "liquid" was brought to solidify between two slabs of crystal with the wanted angular misorientation. The resulting grain boundaries are not straight, and their structure cannot be described within the rigid framework of the coincidence-boundary theories. An example is shown in fig. 2. The heavily distorted layer along the boundary is narrow (a few atomic layers thick), which is in agreement with the traditional ideas of the structure of grain boundaries.

The two-phase materials investigated are dispersion-strengthened materials and fibre composites. The high-temperature stability of the stainless steel dispersion-strengthened with aluminium oxide that has been developed at the Metallurgy Department (Risø Report No. 225 (1970) p. 25) was examined; the dispersoid particles, the grains, and the subgrains were found to remain almost unchanged after prolonged annealing at 900°C. The high-temperature stability of a close network of grain boundaries and subgrain boundaries is expected to suppress the void formation and hence the swelling under fast-reactor conditions. Irradiation experiments at 600°C in a high-voltage electron microscope (carried out in collaboration with the AERE, Harwell) show that the number of voids is drastically reduced in the dispersion-hardened materials as compared to the same type of steel produced by casting.

The recrystallization of aluminium/aluminium-oxide alloys with low oxide content was studied together with the Danish Engineering Academy. The variables investigated were oxide content, oxide distribution, and degree of cold work. The results indicate that particle spacing and degree of cold work are the important parameters for the recrystallization behaviour of these dispersion-strengthened materials.

The densification of mixtures of metal powder and powder of ceramic particles by compaction and sintering and its relation to the morphology of the powders, were studied with reference to the production of dispersion-strengthened materials.

The fibre-composite projects reported under this heading refer to copper reinforced with tungsten fibres. For small fibre spacings it has been observed that the strength and the elongation of the composites are different from those calculated from the simple law of mixtures that seems to apply for larger fibre spacings. For the further investigation of this phenomenon it is important to know the exact properties of fibres and matrix. Therefore individual fibres were tensile-tested, and different ways of measuring Young's modulus for the copper matrices of different samples were investigated. The modulus differs from sample to sample, because the matrix is normally a single crystal.

Within fracture mechanics the acoustic emission technique was successfully applied during testing to failure of concrete lids (carried out by the Engineering Department at Risø). There was a convincing correlation between the acoustic activity and the occurrence of cracks in the concrete. For the evaluation of irradiation damage in steel, measurements of the acoustic attenuation at 1 2 MHz were carried out at different temperatures. As to a possible correlation between the acoustic attenuation and the brittle/ductile transition the experiment has, so far, not been conclusive. Equipment for the measurement of crack-opening displacement (to be carried out in collaboration with Det Danske Staalvalseværk) was constructed. It is to be mounted on a tensile testing machine at Det Danske Staalvalseværk.

In the field of zirconium alloys the precipitation reactions in a Zr-Cr-Fe alloy (Zr-2% Cr -0.16% Fe) were followed by resistivity measurements. The starting material was solution-treated and then quenched to produce a mixed structure of Widmanstätten α-phase and twinned martensite. The precipitation of two distinct phases was detected during low-temperature ageing. They were of a type similar to the θ' precipitates in the aluminium-copper system. In an investigation of the ductility of hydrided zircaloy-2 the tensile results were computer-analysed. The variation of $d \log \sigma_t / d \log \varepsilon_t$ versus $\log \varepsilon_t$ (σ_t is the true stress, ε_t the true strain) was found to give a better indication of the transition from discontinuous to smooth yielding than the σ-versus-ε curve normally applied. Discontinuous yielding was promoted by increasing strain rate and suppressed by increasing hydrogen content.

A model for the influence of intermetallic compounds on the oxidation of zirconium alloys was proposed. The basic idea is that the oxidation of the intermetallic particles produces a volume expansion leading to cracks in the zirconium-oxide film. These cracks will facilitate oxygen diffusion and hence accelerate corrosion.

Materials Development

Various advanced zirconium alloys were examined with respect to fabrication variables, mechanical properties, irradiation behaviour, and corrosion resistance.

The work on zircaloy-2 dispersion-strengthened with yttria continued in collaboration with the UKAEA (RFL, Springfields). The alloys were creep-tested from room temperature to 600°C, corrosion-tested in steam at 400°C, and a number of alloys were exposed to neutron irradiation followed by tensile testing. The results so far show that the dispersion-strengthened alloys exhibit good thermal and irradiation stability, twice the strength of zircaloy-2, and a corrosion stability comparable to that of zircaloy-2.

For the zirconium alloys investigated in collaboration with the UKAEA, the AB Atomenergi, Sweden and the IFA, Norway, the iso-thermal and iso-chronal annealing behaviour was established with reference to the heat treatment of the first experimental batches of tube material. Several of the alloys showed at least as good corrosion behaviour as zircaloy-2 even though they had not received the heat treatment thought to give optimum corrosion resistance. All of the alloys showed a considerably better resistance to grain growth than zircaloy-2.

The German low-alloy steel BH 70 was submerged-arc-welded in collaboration with the Danish Welding Institute, and test specimens for impact testing of weld metal and heat-affected zones were exposed to neutron irradiation under PWR (6×10^{19} n/cm^2 290°C) and BWR (5×10^{18} n/cm^2 265°C) conditions. The increase in transition temperature was found to be largest for the PWR condition, and is believed to be associated with a relatively high copper content of 0.25% in the weld metal compared to 0.16% in the base metal[x]. The high copper content in the base metal is due to the use of copper-clad electrodes.

---

[x] Welding Research Suppl. 1970: 49:10 pp. 953_s-460_s.

Nickel-base material reinforced with fibres of tungsten for use at high temperatures (1000°C) was examined partly as contract work for the NORDFORSK project committee for metallic composites. The work was concentrated on production of nickel-tungsten composites by casting of nickel around a bundle of tungsten fibres. The specimens produced in this way showed constant fiber diameter and hence constant volumen percentage over a length of 70 mm. The specimens have been used for mechanical testing and oxidation testing at a number of laboratories in Scandinavia.

Experiments with transformation of scale from steel production into iron powder are being carried out together with an economic evaluation of the process.

Materials Technology

Equipment for brazing of small work pieces was developed. The brazing can be carried out either in vacuum or in hydrogen atmosphere and as heat sources can be used either a resistance furnace of a 12 kW high-frequency furnace.

A new procedure for brazing Inconel 718 with nickel as braze material was established. The procedure makes it possible to braze several joints in the same operation, for example a spacer for fuel elements with 49 joints (see fig. 4).

The experiments carried out in order to establish a general procedure for testing shear, fatique, and impact strength of different brazed joints were continued. Closer tolerances were obtained by changing the procedure for the machining of specimens, and a computer code proved very useful in analysing the test results.

The work on methods for non-destructive testing of products was concentrated on the construction of equipment for the measurement of dimensions and the control of defects in zircaloy fuel tubing. During the first phase of this programme the work was mainly assessment of solutions to key problems such as the mechanical construction of the rotating measuring device, signal transmission, tube guides, etc. From the analysis the optimum solutions were chosen and construction of the equipment was initiated. A prototype unit was presented at the "Nuclex 72 Fair" in Basle, Switzerland.

For checking of fuel element profiles before and after irradiation two identical profilometer benches were constructed. The two benches have now been calibrated, and preliminary results indicate that the uncertainty on the measurements is less than 10 μm over the whole length (2 m).

Fig. 3. A specimen consisting of 500 μm diameter fibres of W-3%Re in a matrix of nickel after tensile testing. The fibres (vertical) show multiple fracture (horizontal black marks). The distribution of lengths of broken fibre can be used to estimate the strength of the bonding between matrix and fibres.

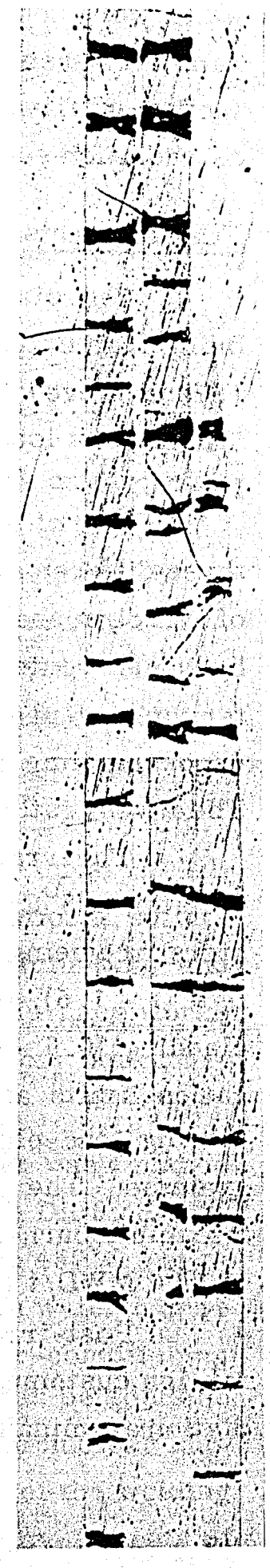

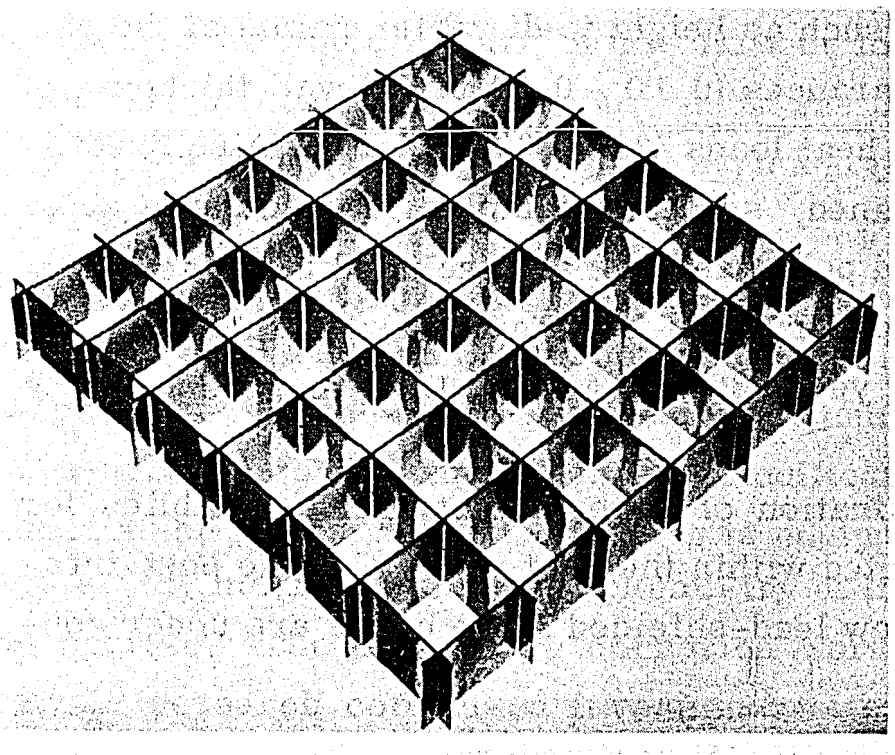

Fig. 4. Spacer of inconel 718 brazed in vacuum.

The experimental part of the densitometric scanning of X-ray films of flat fuel plates was terminated. The aluminium thicknesses corresponding to lower and upper tolerance limits for the uranium content in a fuel plate were found by means of termoluminiscent dosimeters. The method can now be used in production. Experimental work was initiated on the detection of flaws in heavy metal sections, using Risø's linear accelerator as radiation source.

Fuel Elements

The six Danish UO_2-zircaloy test fuel elements that are at present being irradiated in the Halden BWR, Norway, had at the end of December 1972 achieved burn-ups in the range from 7,000 to 23,900 MWD/t UO_2. The highest local burn-up, namely 29,400 MWD/t UO_2, was obtained in the IFA 161.

One of the unloaded assemblies, IFA 162, contained fuel pins given three different surface treatments. Preliminary results from the analysis of hydrogen and deuterium content in the cladding are given in table I. The hydrogen content seems reasonable, whereas the measurements of deuterium content give unexpectedly high results in view of the relatively short exposure time (220 days at power, average burn-up 5,600 MWD/t UO_2). The investigations are being continued.

The irradiation of UO_2-Zr test fuel pins at nominal BWR conditions (70 atm, 285°C) continues in the DR 3 reactor. A large number of parameters are being investigated, such as height to diameter ratios of the pellets (1 - 1.5), pellet-clad clearances (0.10 - 0.34 mm), wall thickness of cladding (0.6 - 0.8 mm), and heat loads (300 - 900 W/cm). Also specification limits are being examined, so that examples of rejectable autoclaving, end-plug welding, and pellet surface are included in the test programme. The status of the programme is summarized in table II. The maximum burn-up obtained as yet is 30,800 MWD/t UO_2, and the target is 40,000 MWD/t UO_2.

Post-irradiation examination of several test fuel assemblies for foreign customers was completed within the past year. For the post-irradiation examination work six new lead-shielded glove boxes are under con-

Table I

Gas analysis of IFA 162 zircaloy cladding

No. of samples analyzed	Autoclaving of inner and outer surface (hours)	Range of results	
		H (ppm by wt.)	D (ppm by wt.)
7	none	40-65 (1 at 75)	55-70
16	24	50-90 (1 at 105)	85-165 (2 at 190)
2	72	35-75	90-110

Table II

Summary of fuel pin irradiations in the DR 3
(December 1972)

Burn-up (MWD/te UO_2)	Number of pins	
	Unloaded	In reactor
< 1,000	19	-
1,000- 5,000	18	8
5,000-10,000	7	2
10,000-15,000	3	-
15,000-20,000	1	-
20,000-25,000	-	4
25,000-30,000	-	3
>30,000	-	3
Total	48	20

struction in the hot cells. The boxes are applicable for work on plutonia-containing materials. An apparatus for vacuum-impregnation with hardenable resins of porous fuel was developed. By this method a complete filling of pores and cracks is obtained. Also new equipment for determination of internal pressure and free volume of fuel pins was constructed. The uncertainty on the determinations with this apparatus is of the order of 2%.

Two special fuel elements for the DR 2 test reactor were produced in collaboration with the Elsinore Shipbuilding and Engineering Co., Ltd.

As a result of the programme on casting of U-Al alloys, a chill mould[x] was developed which has the advantage of giving a uniform solidification of the liquid metal. A new furnace for oxidation, calcination, and reduction of uranium oxide compounds was installed. The furnace works continuously with a capacity of 6-10 kg/h and gives a satisfactory uniformity of the resulting powder.

A rig for in-pile corrosion testing of zirconium alloys was finished and has, after a few modifications, been commissioned in the DR 3. Steam may be used as the corrosive medium at temperatures up to 450°C and at pressures up to 80 atm. A minor modification after which water can be used in the rig is planned. The rig is equipped with a water-conditioning system by means of which the chemistry of the feed water can be adjusted as desired. The out-of-pile corrosion work in the field of nuclear materials research comprised investigations of the influence of the welding atmosphere on the corrosion resistance of welds in zircaloy-2, tests of corrosion resistance of components for fuel elements (spacers, springs, etc.), and various problems with regard to the water chemistry at a possible change from BWR to PWR conditions for forth-coming fuel element irradiations in the DR 3.

[x] Patent applied for

TRANSMISSION ELECTRON MICROSCOPY OF CREEP-DEFORMED MAGNESIUM OXIDE

J. B. Bilde-Sørensen

In the past decade there has been a growing interest in the high-temperature creep of ceramic materials. However, most of the experimental work described in the literature has concentrated on the dependence of creep rate upon parameters such as stress, temperature, and grain size. Structural examinations have with a few exceptions only comprised optical microscopy.

In several creep reviews it has been shown that the secondary (steady-state) creep rates of many materials depend linearly on stress if the stress and grain size are both sufficiently low. At higher stresses and/or grain sizes the dependence of creep rate upon stress follows a power law.

The most probable interpretation of creep with linear stress dependence is some sort of Nabarro-Herring creep, where the rate-controlling mechanism is vacancy diffusion from grain boundaries under tension to grain boundaries under compression. In contra-distinction to this, it is a general assumption that the deformation mechanism in the power law range is some sort of diffusion-controlled dislocation movement, so knowledge of the dislocation structure of ceramics deformed in this range is very much needed.

We decided to study the dislocation structure of creep-deformed polycrystalline magnesium oxide by transmission electron microscopy (TEM). Stresses and grain sizes were chosen so that secondary creep took place in the power law range, and we confined ourselves to studying the structure in specimens from tests that had been interrupted in the secondary part of the creep curve.

MgO was chosen for the investigation because it has a simple crystal structure, because it can be produced with almost theoretical density by hot-pressing, and because it is relatively easy to produce satisfactory thin foils from this material.

The thin foils for TEM were produced by purely chemical thinning in a hot (135°C) mixture of 99 volume parts 70% H_3PO_4 and 1 volume part concentrated H_2SO_4. Before the specimen was inserted in the microscope, a thin layer of carbon was vacuum-deposited on the surface. This was done in order to avoid charging of the specimen when it was hit by the electron beam.

Subgrain Boundaries

When MgO is creep-deformed, the single grains are divided into more or less well-defined subgrains. In the electron microscope we see three different types of subgrain boundaries. These are shown in figs. 5-7. Fig. 5 shows a boundary consisting of an array of parallel dislocations. In fig. 6 the boundary is formed by two different sets of parallel dislocations crossing each other. An analysis showed that the Burgers vector of dislocations in one set formed an angle of 90^{o} with the Burgers vector of dislocations in the other set. If one examines the points of intersection, it is seen that no reaction between dislocations from the two sets can be detected. Actually a reaction between dislocations with mutually perpendicular Bur-

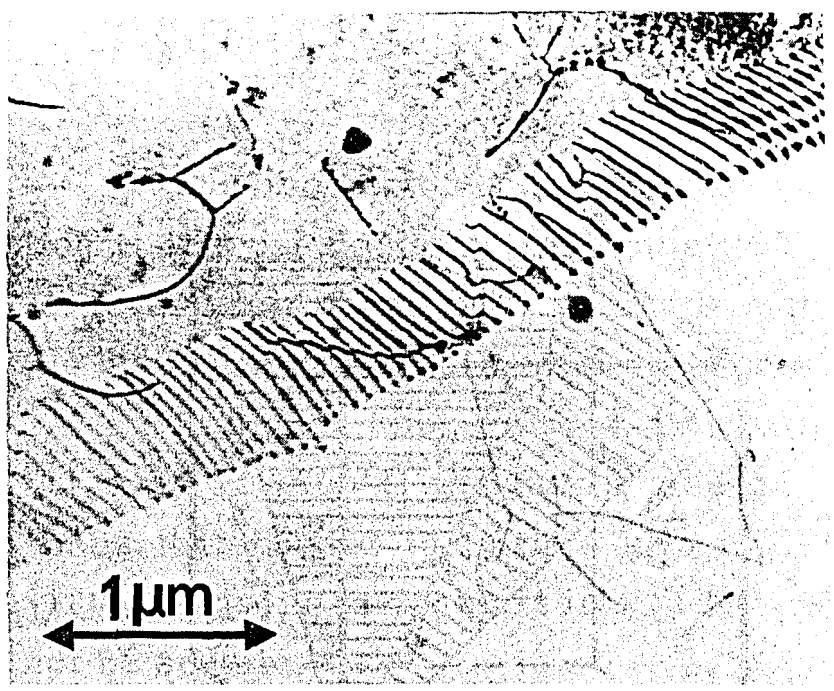

Fig. 5. Subgrain boundary consisting of parallel dislocations.

Fig. 6. Subgrain boundary formed by two sets of parallel dislocations whose Burgers vectors are mutually perpendicular.

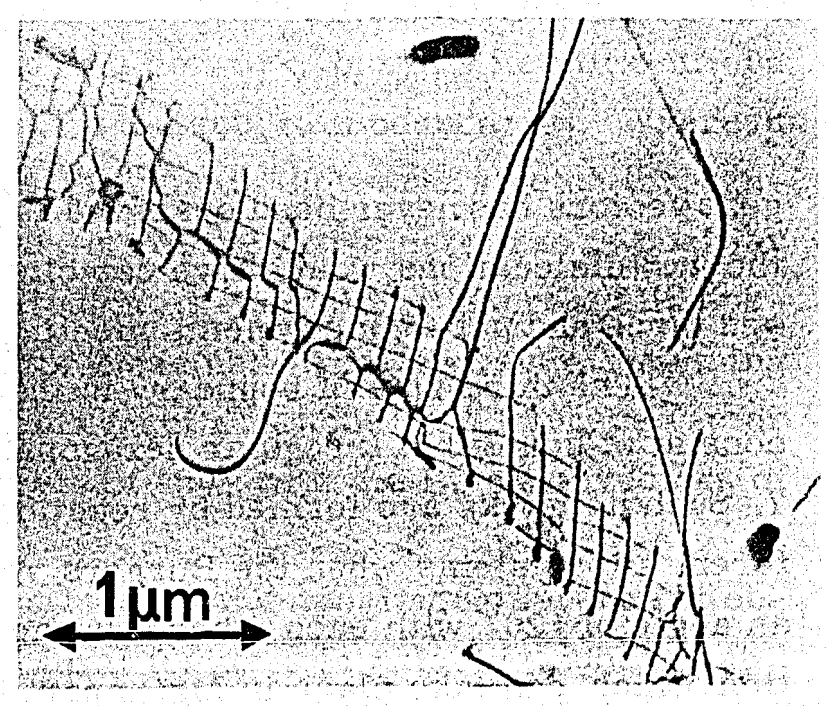

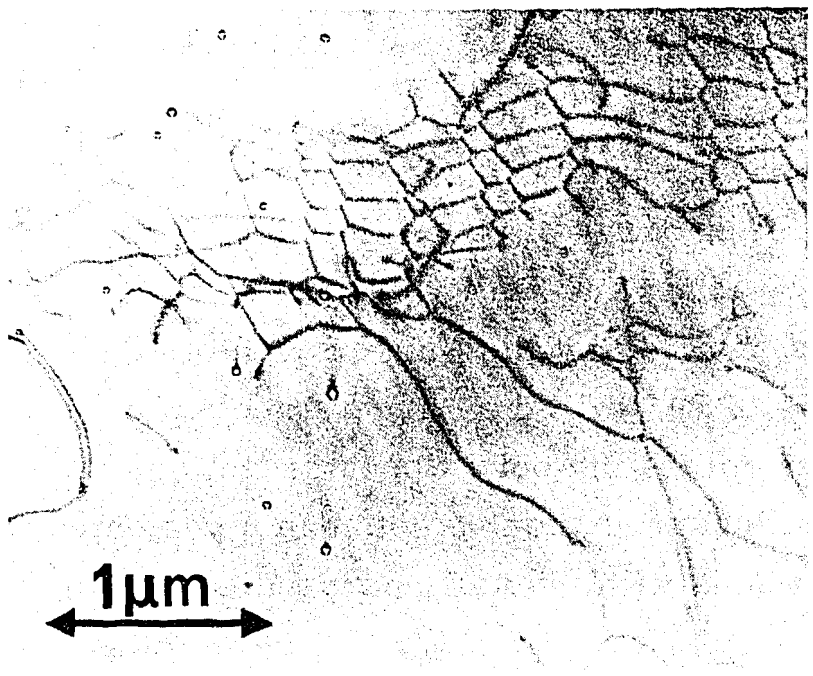

Fig. 7. Subgrain boundary consisting of a somewhat irregular hexagonal network, formed by a "120°-reaction".

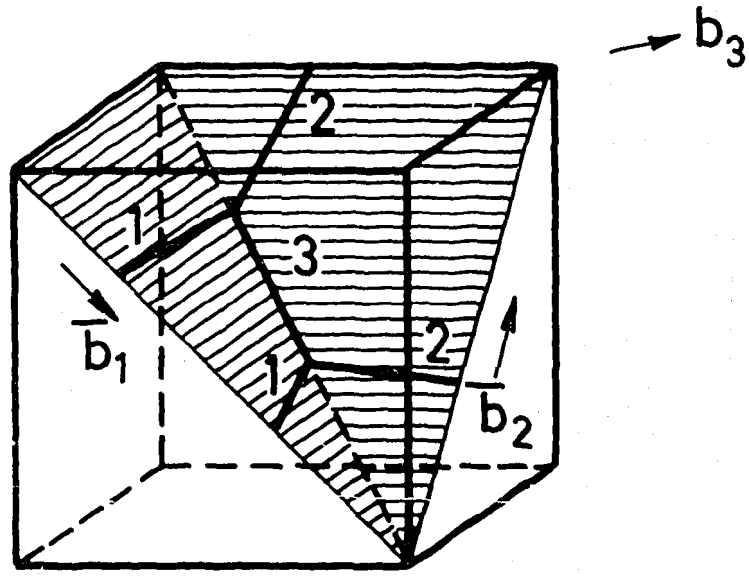

Fig. 8. Schematic representation of the "120°-reaction".

gers vectors has never been observed in MgO. If a reaction had occurred, the two dislocations would have combined over some length, and we would see three and not four segments meeting at each node.

The third type of boundary is the most common. These boundaries consist of somewhat irregular hexagonal networks as the one shown in fig. 7. Such networks are formed by reactions between dislocations in two different slip systems when the Burgers vectors of the two dislocations form an angle of 120° with each other. In fact this is the only dislocation reaction which can take place in MgO apart from the annihilation of two dislocations of opposite sign. One may in passing notice that in both figs. 5

and 6 a "120°-reaction" - as we shall call it in the following - has taken place locally between dislocations in the boundary and a "foreign" dislocation, so that the formation of a hexagonal network has been initiated.

The "120°-Reaction"

Fig. 8 shows a sketch of the "120°-reaction". Normally, dislocations in MgO slip over {110} planes in ⟨110⟩ directions. In fig. 8 we have drawn a dislocation (1) in the (011) plane with a Burgers vector $\bar{b}_1 = \frac{a}{2}[01\bar{1}]$. This dislocation has reacted with a dislocation (2) with $\bar{b}_2 = \frac{a}{2}[\bar{1}01]$. Dislocation (2) glides in the (101) plane. The two slip planes intersect along [111], and the new dislocation (3) will therefore lie along this line. We find its Burgers vector $\bar{b}_3$ by adding $\bar{b}_1$ and $\bar{b}_2$:

$$\frac{a}{2}[01\bar{1}] + \frac{a}{2}[\bar{1}01] \rightarrow \frac{a}{2}[\bar{1}10].$$

The line vector $\bar{\xi}_3$ and the Burgers vector $\bar{b}_3$ of the new dislocation are perpendicular to each other, so the dislocation is of the edge type. However, the plane (112) determined by $\bar{\xi}_3$ and $\bar{b}_3$ is not a slip plane, so the dislocation is sessile, i. e. it cannot move by slip, but only by climb.

At higher temperatures dislocations may also slip in {100} planes, but even at 1600°C the stress needed to initiate slip in {100} is about 3 times that needed to initiate slip in {110}. If a dislocation gliding in a {100} plane is taking part in a "120°-reaction", the reaction product will not be sessile.

Structure Inside the Subgrains

Inside the subgrains we find a structure as shown in fig. 9. The dislocations are also here arranged in a network, but this network differs in many respects from those we saw in the subgrain boundaries. Whereas the boundary networks are rather flat, the "inside" networks stretch throughout a whole subgrain. Also the mesh size of the latter networks is coarser and the structure more irregular, indicating that more different slip systems are operating in the formation of these networks. However, one thing is common: where three dislocations meet at a node, the Burgers vector of one dislocation must form an angle of 120° with the Burgers vectors of the two others.

It is important to note that pile-ups or entanglements were not observed. The existence of these structural features is namely a fundamental assumption in several creep models which are appreciably invalidated by

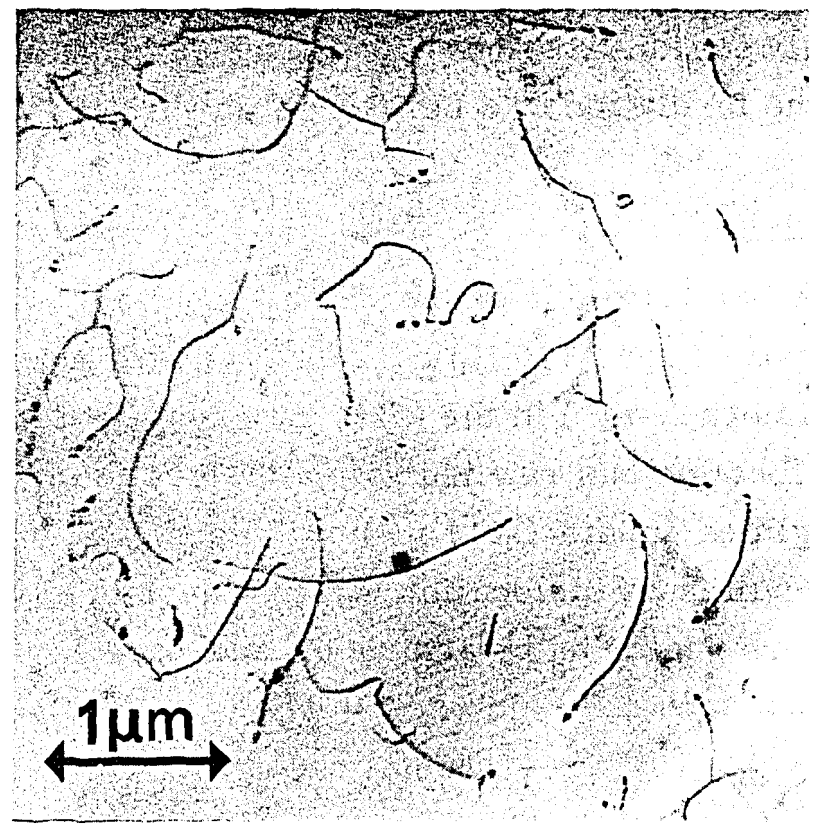

Fig. 9. Typical dislocation structure inside the subgrain boundaries.

the lack of such features. Loops are seen occasionally although they cannot be considered a typical trait of the structure. Dipoles are seldom seen.

We have now described the dislocation structure qualitatively. Quantitatively we investigated the dislocation density, the character of the dislocations, and the segment length distribution.

Dislocation Density

Dislocation densities were measured by counting intersections between dislocations and surfaces per unit area. This method is similar to the etch pit technique used in optical microscopy, but in the case of TEM, a correction must be made for dislocations out of contrast. Dislocations are namely invisible if $\bar{b} \cdot \bar{g} = 0$ and $(\bar{b} \times \xi) \cdot \bar{g} \lesssim 0.64$ are both fulfilled. $\bar{g}$ is here the so-called reflection vector. The correction was made by multiplying the counted number of dislocations by $\frac{6}{5}$ when the reflection vector was of the $\langle 220 \rangle$ type (corresponding to an invisible fraction of $\frac{1}{6}$), by $\frac{3}{2}$ for $\bar{g}$-vectors of the $\langle 200 \rangle$ type, and so on.

For most creep-deformed metals it is found that the dependence of dislocation density ρ upon stress σ follows the relation $\rho = (\frac{\sigma}{\alpha b G})^2$, where G is the shear modulus and α a numerical constant near unity. We found that this relation also holds for MgO. The densities are here given as cm/cm^3 (volume density) which is twice the measured quantity, dislocations/cm^2 (area density).

Character of the Dislocations

The character of the dislocations was found by a simultaneous determination of the Burgers vector and the crystallographic direction between the two end points (nodes or intersections with the surfaces) of the dislocation in question. One micrograph with the dislocation out of contrast was used for the determination of the Burgers vector. Two other micrographs, where the dislocation was visible, were used to find the direction between the end points. These two micrographs were taken with the specimen in different orientations.

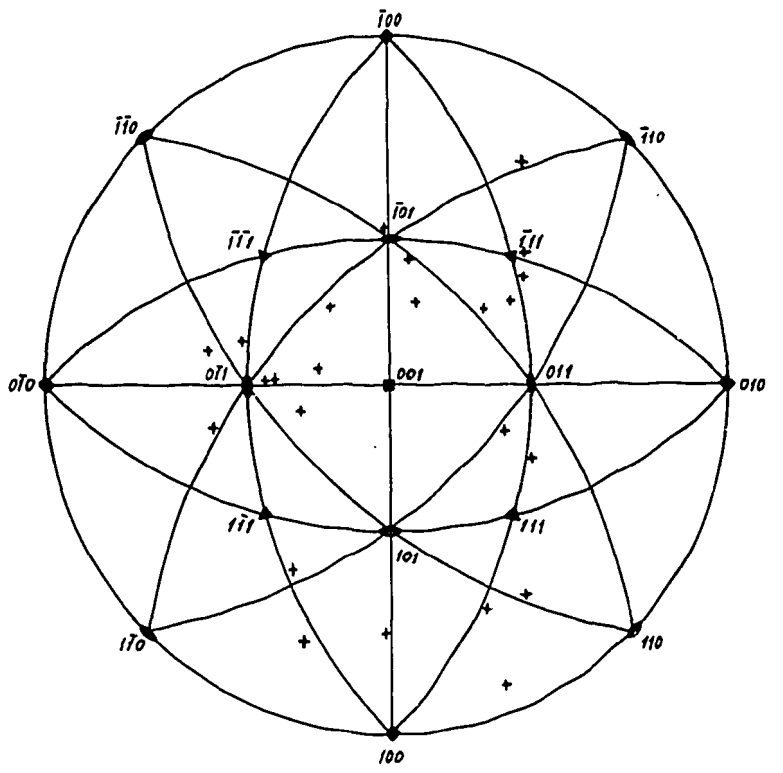

Fig. 10. Stereographic projection of dislocation directions for $\bar{b}$ normalized to a/2[011].

A stereographic projection of the directions of the dislocations is shown in fig. 10 for $\bar{b}$ normalized to $\frac{a}{2}[011]$. In such a projection points represent directions. The circle arcs we have drawn represent planes. The arc running through $[\bar{1}00]$ and $[011]$ is the $(0\bar{1}1)$ plane which is the slip plane. Several dislocations are within the experimental error situated in this plane. They are in other words glissile. Others are situated in the climb plane (011) (through $[\bar{1}00]$ and $[01\bar{1}]$). The climb plane is the plane in which pure edge dislocations - as for instance those formed by the "120^{o}-reaction" - will climb. Still others are scattered over the projection. These dislocations can be interpreted as mixed dislocations that have climbed out of their slip plane.

One should not attach too great significance to the ratio between glissile and sessile dislocations. Geometrical considerations show that under the experimental circumstances used, there may have been a greater than random chance of picking sessile dislocations for the investigations.

Dislocation Segment Length Distribution

The measurement of the dislocation segment length distribution is only preliminary. By segment length we mean in this context the distance between two nodes to which the segment in question is tied. The method is based on the measurement of projected lengths of all whole segments (i. e. segments tied to two nodes both situated in the foil) in a foil with known thickness. This two-dimensional distribution is then by computer calculations transformed into a three-dimensional distribution. We found that the cumulative distribution is well described by the equation

$$C(L) = \frac{1}{2}\left[1 + e^{-0.44\left(\frac{L}{L_{av}}\right)^{-1.66}} - e^{-0.93\left(\frac{L}{L_{av}}\right)^{1.83}}\right],$$

where C(L) is the fraction of segments with a length of less than L_{av} and R is the average segment length. The distribution is plotted in fig. 11.

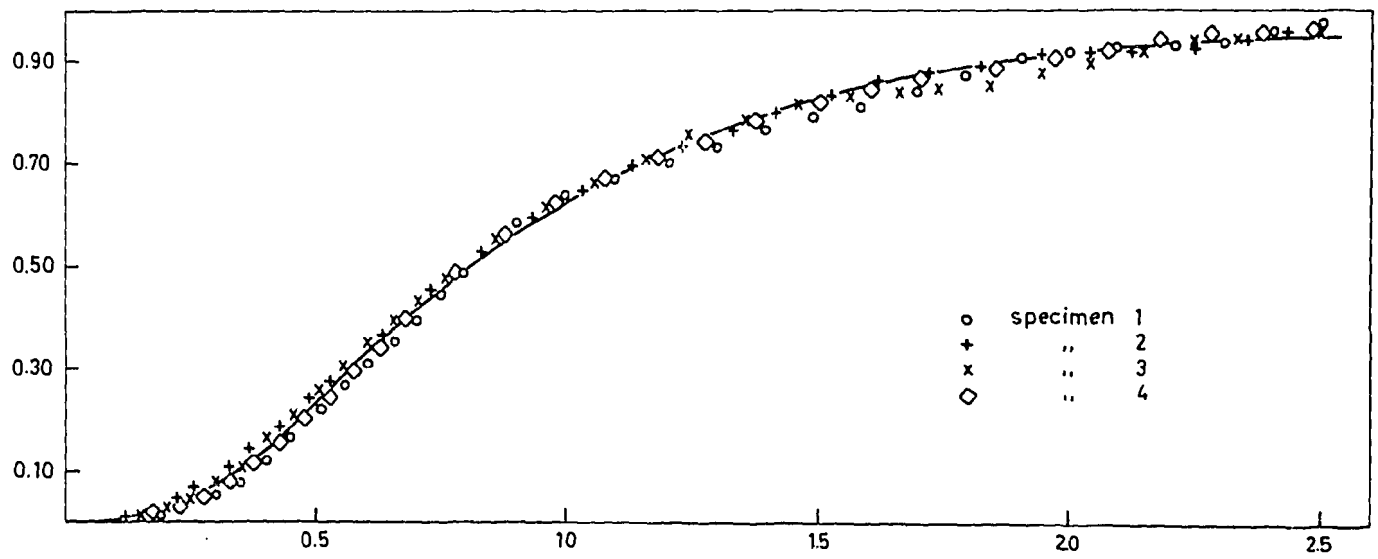

Fig. 11. Cumulative dislocation segment length distribution.

Conclusion

On the basis of the structural investigation we propose a model for the creep of MgO. It would, however, be outside the scope of this article to go into a detailed discussion of this model. The detailed considerations may be found elsewhere[x]. The main points of the model are that the decrease in the number of segments by annealing is balanced by the increase caused by reactions between glissile dislocations, and that slip gives the main contribution to the deformation although the rate of slip is controlled by the annealing of the dislocation network and thus by diffusion. The creep rate expected from a semiquantitative estimate and the experimental rates agree within one order of magnitude.

x) J. B. Bilde Sørensen, J. Am. Cer. Soc. 55 (1972) 606-610.

In conclusion it should be emphasized that our model only gives a broad outline of the creep phenomenon. Many finer details are not fully understood. Particularly the model cannot explain the presence of the sub-grain boundaries, and their possible influence on the creep rate is ignored. However, this shortcoming is shared with other creep models and for that matter with tensile test theories, too. The knowledge of creep in MgO as well as in other materials is far from complete, and much work has still to be done.

DETERMINATION OF THE INTERNAL FREE VOLUME AND PRESSURE OF IRRADIATED ZIRCALOY CLAD URANIUM-DIOXIDE FUEL PINS

C. Bagger and K. Bryndum

Fuel elements for light-water-cooled reactors consist of a number of fuel pins. The fuel, which is sintered uranium dioxide pellets, is contained in zircaloy tubes. The length of the tubes may be as much as 4 metres, and the diameter is in the range 10 - 15 mm.

To design a fuel pin and to evaluate its performance it is essential to know the internal pressure and the amount of gaseous fission products generated during the irradiation. During post-irradiation examination, the amount of gas in the internal free volume can be determined by piercing the pin and extracting the gas for measurement. A technique has been established that combines the measurement of the gas content with a determination of the free volume. It is thus possible to calculate the internal pressure.

Equipment

The equipment we use at Risø consists of an in-cell piercing unit, connected to a gas-extracting and -measuring system placed outside the cell in a perspex glove box.

Fig. 12 shows the piercing unit. The pin is locked in a horizontal position under the piercing head, which is lowered until a tight seal is obtained with an O-ring glued into the bottom part of the unit. After evacuation of the extraction system and the piercing head, we pierce the pin by forcing a hardened steel needle with triangular cross section through the

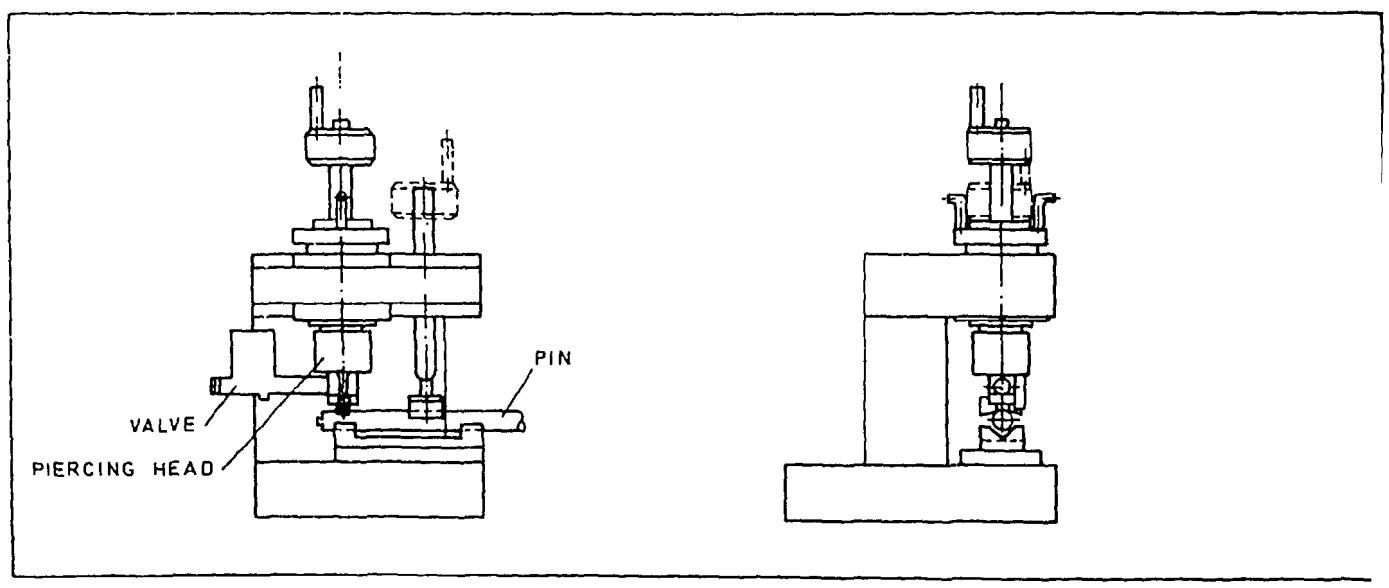

Fig. 12. Piercing unit.

cladding. The extraction system is shown in fig. 13. The extraction is performed with a mercury diffusion pump and a Toephler pump. Extracted gases are transferred for measurement to a system of calibrated bulbs connected to a manometer.

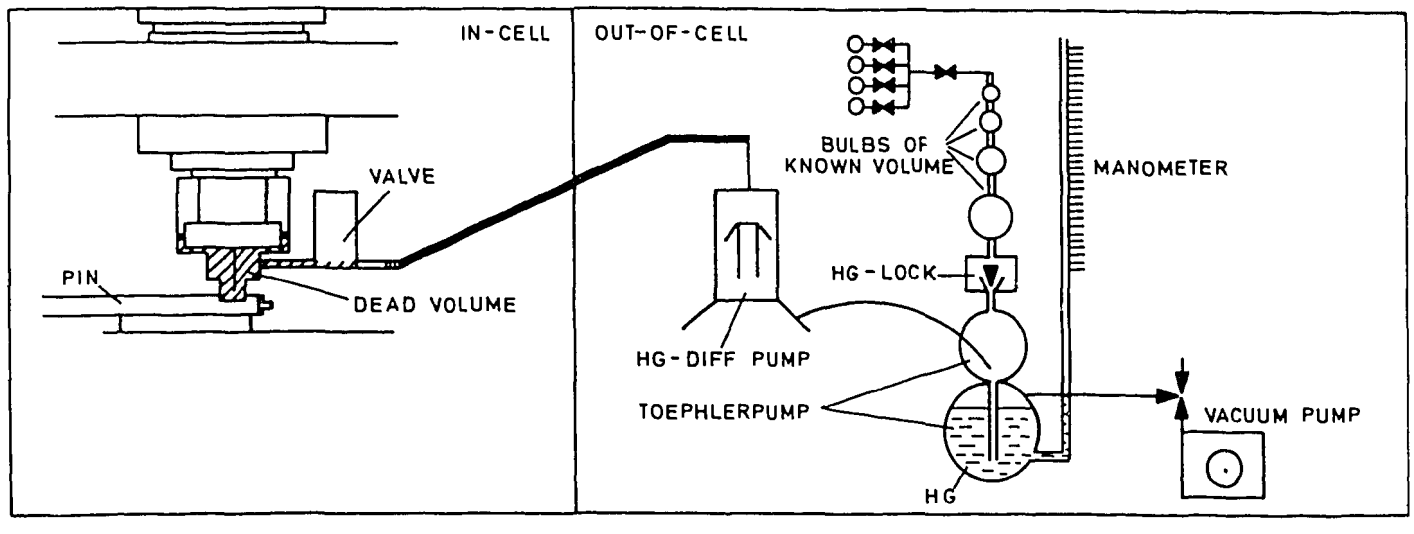

Fig. 13. Gas sampling system.

Technique

The technique is a three-stage procedure:

Stage 1: After evacuation of the system, the pin is pierced and the gas is transferred to the calibrated bulbs. Volume and pressure are read.

Stage 2: The pin, the piercing head, and the connecting lines are filled with helium until atmospheric pressure is obtained. To separate the pin from the extracting system we close a valve in the piercing unit. The rest of the extraction system is evacuated, thus leaving helium at atmospheric pressure in the pin and the dead volume of the piercing unit between the pin and the valve. This dead volume has previously been calibrated.

Stage 3: The valve is opened and the helium is transferred to the calibrated bulbs. Pressure and volume are read.

Theoretical Basis for the Measurements

The following symbols are used:

P_1 = original pressure in the pin
V_1 = free volume of the pin
P_2 = pressure of fission gas in the bulbs
V_2 = volume of fission gas in the bulbs
P_3 = pressure of He in the pin
V_3 = dead volume of the piercing unit
P_4 = pressure of He in the bulbs
V_4 = volume of He in the bulbs.

The result are derived in the following way:

From stage 1 the following equation is obtained:

$$P_1 \times V_1 = P_2 \times V_2. \tag{1}$$

From stage 3 is obtained:

$$P_3 \times (V_1 + V_3) = P_4 \times V_4. \tag{2}$$

By combination of (1) and (2) the following expressions are derived for V_1 and P_1:

$$V_1 = \frac{P_4 \times V_4 - P_3 \times V_3}{P_3}. \tag{3}$$

Because of the limited size of the measuring bulbs it is necessary to perform the measurements of the large quantities of gas extracted from V_1 and V_3 in more than one turn. These successive measurements cause a decrease in the accuracy which is reflected in the vertical steps on the curves in fig. 14. It is seen that the dead volume should be minimized. Therefore, the valve should be placed as close to the pin as possible. The optimal solution would be to isolate the pin by closing the piercing hole during the evacuation, prior to helium-extraction.

We chose atmospheric pressure for helium-refilling because of the possibilities of exact determination of pressure from a precision barometer, and in order to avoid in-leak or out-leak from the pin while the system was being prepared for helium-extraction. The accuracy will be slightly

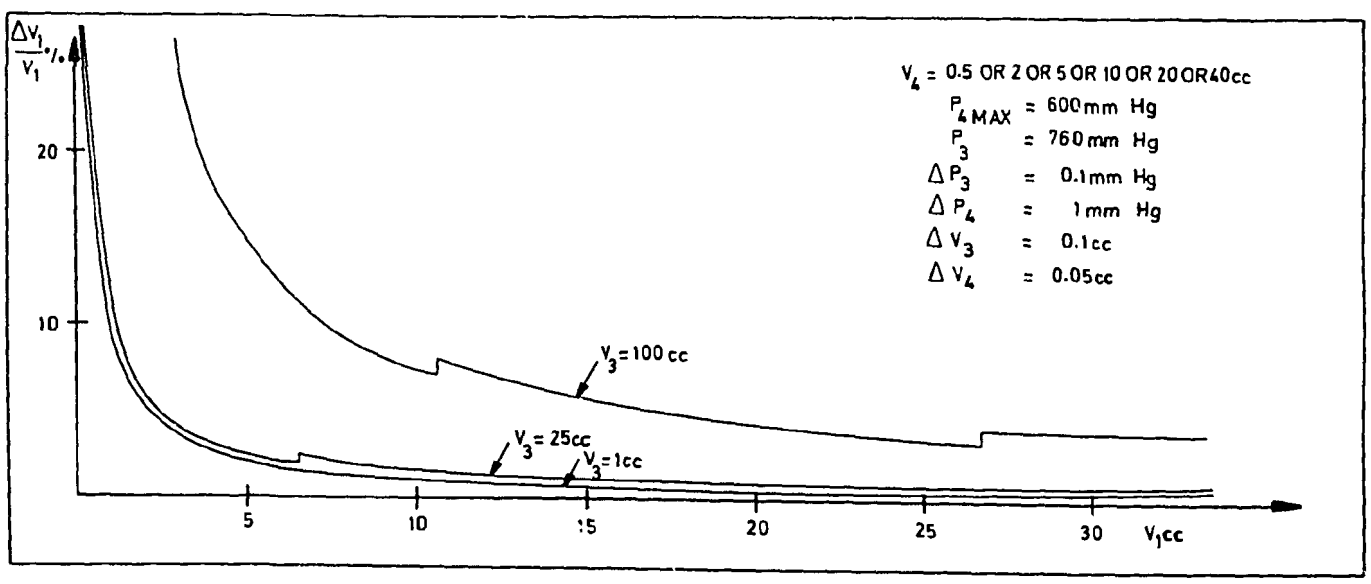

Fig. 14. $\Delta V_1/V_1 = F(V_1)$ for different dead volumes (V_3).

improved if a refilling pressure of the same magnitude as the initial pressure in the pin is used, provided that the uncertainty of the pressure measurement is not changed and that the in-leak or out-leak does not change.

Because of the time used for non-destructive testing, almost all fuel test pins examined at Risø had a cooling period long enough for them to reach ambient temperature. If the cooling time was so short that the pin had not reached ambient temperature, efforts were made to secure that the refilled helium reached the temperature of the pin before the valve was closed and the rest of the system evacuated.

Equations (1) and (2) are in this case modified to:

$$\frac{P_1 \times V_1}{T_1} = \frac{P_2 \times V_2}{T_2} \tag{4}$$

$$\frac{P_3 \times V_1}{T_1} + \frac{P_3 \times V_3}{T_2} = \frac{P_4 \times V_4}{T_2} . \tag{5}$$

T_1 is the temperature of the pin, and T_2 is the temperature of the extraction system. This gives the following expressions for V_1 and P_1:

$$P_1 = \frac{P_4 \times V_4 - P_3 \times V_3}{P_3} \times \frac{T_1}{T_2} \tag{6}$$

$$P_1 = \frac{P_2 \times V_2 \times P_3}{P_4 \times V_4 - P_3 \times V_3} . \tag{7}$$

This means that, without considering the temperature of the pin, we were able to determine the total amount of gas ($P_2 \times V_2/T_2 \times R$) and the internal pressure (P_1) for a pin which had not reached ambient temperature. If a determination of the internal free volume is needed, corrections should be made for the pin temperature. This temperature may be calculated from irradiation data and cooling time, or it can be measured directly.

The hotter pin surface constitutes only a small part of the limiting surface of the dead volume, and mixing of gas from the pin and the dead volume occurs through a small hole. Therefore, the temperature of the gas in the dead volume was regarded as T_2. However, a small, unknown rise in the temperature of the gas in the dead volume may be expected. This emphasizes the demand for a dead volume as small as possible. Our present apparatus has a dead volume of 7.72 cm^3.

Results

We pierced 10 test pins with an internal free volume of 2.5 - 3 cc and a burn-up of 800 - 1200 MWD/t, and compared the measured volumes to the internal free volumes calculated from the fabrication data. We chose these pins for the comparison because no major changes are to be expected at this low burn-up. The differences between measured and calculated values were in nine cases within the expected limits.

New equipment is under construction. With an appropriate design of piercing head and valves we succeeded in reducing the dead volume to about 2 cm^3. A further reduction in the size of the dead volume is not necessary because the uncertainty of the volume measurement will now be of the same size as the uncertainity in the calculation of the initial pin volume.

PARTICIPATION IN INTERNATIONAL COLLABORATION

The department is engaged in the following types of international collaboration: joint technical projects, committee work, reception of research fellows, and technical and scientific meetings.

Participation in the NEA reactor project at Halden was continued. Six Danish fuel elements are at the moment being tested under irradiation in the Halden reactor. In the hot cells at Risø elements of other signatories (Italy and Japan) irradiated at Halden were examined. The participation in the NEA reactor project Dragon was continued.

Joint technical projects were continued on measurement of the thermal conductivity of uranium dioxide under irradiation, studies of the thermodynamic behaviour of uranium-dioxide/plutonium-dioxide mixtures, and irradiation in the DR 3 of zircaloy-clad uranium-dioxide/plutonium-dioxide fuel rods (with AB Atomenergi, Sweden). Also the programme on dispersion-strengthened zirconium alloys (with the UKAEA) was continued with testing of other dispersants than yttria and other basic materials than zircaloy-2 in order to improve corrosion resistance and neutron absorption characteristics of the alloys. Together with the Atomic Energy of Canada Ltd. (AECL) experiments are planned to investigate the in-pile creep properties of the alloys. The joint programme on examination of advanced zirconium alloys for water reactors (with the UKAEA, AB Atomenergi, and the IFA, Norway) was continued. The department took part in a joint Scandinavian Nordforsk project on fibre reinforcement, and in a Scandinavian working group on hot cell techniques.

The department participated in the Halden Programme Group (member: N. Hansen), in the Halden Project Working Group on Fuel (member: P. Knudsen), in the IAEA working group on "Engineering Aspects of Irradiation Embrittlement of Reactor Pressure Vessel Steels" (member: A. Nielsen), and in the following Technical Commissions of the IIW (International Institute of Welding): Commission I "Gas welding and allied processes", Sub-Commission A "Brazing and surfacing" (member: J. Christensen), Commission IX "Behaviour of metals subjected to welding", and Commission X "Residual stresses and stress relieving. Brittle fracture" (member: A. Nielsen).

Furthermore the department was represented in the CREST (Committee of Reactor Safety Techniques of NEA) working group: "Material and mechanical problems related to the safety aspects of steel components in nuclear plants" (member: A. Nielsen). N. Hansen was a member of the working group under the EEC concerning technological collaboration, especially regarding metallurgy, and O. Toft Sørensen was a member of the council of International Confederation of Thermal Analysis (ICTA).

EDUCATION AND TRAINING

Two members of the scientific staff of the department have been giving regular lectures on materials to students at the Danish Academy of Engineering. Two staff members acted as external examiners at graduate examinations. A course was arranged on advanced metallurgy for mechanical engineers.

In the department a number of students worked on studies in preparation for their bachelors theses. Eight students from the Department of Mechanical Engineering of the Danish Acedemy of Engineering worked on the following projects:

"Precision Casting of Grids for Fuel Elements",
"Economic Evaluation of the Lost Wax Process for Precision Casting",
"Determination of the E-Modulus in a Fibre-reinforced Material",
"Properties and Structure of Tungsten Fibres",
"Construction of Equipment for Tube Burst Testing of Irradiated Fuel Elements",
"Recrystallization of Aluminium/Alumina Alloys",
"Restitution and Recrystallization of Zirconium Alloys",
"Construction of an Apparatus for Bend Testing of Steel".

Two post-graduate students from the Technical University of Denmark worked in the department; one, from the Department of Structural Properties of Materials worked on his thesis:

"Additive Strengthening Mechanisms in Dispersion-Strengthened Products",

and the other from the same department started work on his thesis

"Interactions between Grain Boundaries and Dislocations".

Study groups were arranged in the fields of zirconium alloys, fuel elements, and in physical metallurgy. The following lectures were given by scientists visiting the department:

"Effect of Impurities on the Defect Structure of Oxides and Their Relation to the Oxidation of Metals" (P. Kofstad, Norway),
"Toughness in Fibre-reinforced Materials" (M.R. Piggott, UK),
"The Mechanical Properties of Perfect Crystals" (N.H. Macmillan, UK),

"High-Voltage Electron Microscope" (B. Hudson, UK),
"In-Pile Corrosion of Zirconium Alloys" (R. C. Asher, UK),
"Field Ion Microscopy of Grain Boundaries" (D. A. Smith, UK).
"Aspects of High-Temperature Deformation" (C. Barrett, USA).

Degrees Awarded

N. Hansen was awarded the degree of dr. techn.

J. B. Bilde-Sørensen was awarded the post-graduate degree of lic. techn.

PUBLICATIONS

In Foreign Languages

Metallurgy Department Annual Progress Report for the Period Ending March 31st, 1971 (Risø Report No. 244 (1971) 42 pp.).

E. Adolph and N. Hansen: Dispersion-Strenghtened Zirconium Products for Water-Cooled Reactors (in: Aspects of Research at Risø. Risø Report No. 256 (1972) 53-67).

To improve the strength of zirconium alloys at high temperatures a powder metallurgy process was developed for manufacture of zircaloy-2 dispersion-strengthened with yttria (Y_2O_3). This work was carried out in collaboration with the UKAEA, Springfields.

Alloys with up to 10 volume per cent of yttria were produced in a high-purity argon atmosphere to ensure a very low impurity content in the final material. The alloys were tensile-tested and creep-tested in the range room temperature to 600°C and corrosion-tested in steam at 400°C. Furthermore a number of alloys were exposed to neutron irradiation before testing.

This development resulted in dispersion-strengthened alloys with good thermal and irradiation stability, twice the strength of zircaloy-2, and a corrosion resistance comparable to that of zircaloy-2.

C. Bagger and K. Bryndum: The Determination of the Internal Free Volume and Pressure of Irradiated Uranium Dioxide Zircaloy Clad Fuel Pins (presented at the BNES Conference on Post-Irradiation Examination Techniques, Reading, England, March 1972. Paper No. 28 in proceedings).

A technique for the measurement of free volume and gas pressure inside BWR type fuel pins is described. The method involves piercing the pin and extracting the fission gas into a volume-measuring device. The evacuated pin is filled to a known pressure with helium, and the volume of helium is measured. The internal free volume together with a known unavoidable dead volume can then be determined, and the internal pressure of the extracted fission gases can be calculated from the data obtained. The error of the system is less than 1% for free volumes of approximately 20 cc, and the accuracy improves with larger free volumes.

J.B. Bilde-Sørensen: Dislocation Structures in Creep-Deformed Polycrystalline MgO (J. Am. Cer. Soc. 55 (1972) 606-610).

Secondary creep of polycrystalline MgO with grain sizes of 100 and 190 μm was investigated at 1300° to 1460°C under compressive loads of 2.5 to 5.5 kgf/mm^2. The dependence of creep rate on load follows a power law with an exponent of 3.2 ± 0.3. The process is thermally activated, with an activation energy of 76 ± 12 kcal/mol. The creep rate is independent of grain size. The dislocation structure was investigated by transmission electron microscopy. The total dislocation density follows the relation, $\sigma = bG\sqrt{\rho}$, commonly found for metals. The dislocations form a 3-dimensional network in which many dislocation segments lie in their slip or climb planes. On the basis of this structure, a model is proposed in which glide is the principal cause of deformation but the rate-limiting process, i.e. annealing of the network, is diffusion-controlled. Theoretical estimates and experimental results agree within 1 order of magnitude.

J.B. Bilde-Sørensen: Secondary Creep of Polycrystalline Magnesium Oxide (presented at the Third Nordic High Temperature Symposium, Risø, June 1972. Proceedings to be published).

The secondary creep properties of polycrystalline MgO were investigated at compressive loads between 2.5 and 5.5 kgf/mm^2 and at temperatures between 1300 and 1460°C. The dependence of creep rate upon stress follows a power law with an exponent of 3.2 ± 0.3. The activation energy was found to be 76 ± 12 kcal/mole. No significant difference was found in the creep rates of materials with grain sizes of 100 and 190 μm.

Transmission electron microscopy revealed more or less well-defined sub-grains and a three-dimensional dislocation network inside the sub-grains. Sessile as well as glissile dislocations were seen in this network. The dislocation density followed the relation $\rho = (\frac{\sigma}{bG})^2$ which is commonly found for metals. Preliminary results on measurements of dislocation segment length distribution are given. A creep model is proposed where the main contribution to the deformation comes from glide, but where the rate-limiting process - namely annealing of the network - is diffusion-controlled.

A. H. Clauer: Review of Recent Advances in the Understanding of High Temperature Strength in Dispersion Strengthened Metals (invited lecture held at the Third Nordic High Temperature Symposium, Risø, June 1972. Proceedings to be published).

Steady Progress is being made in characterizing the high temperature deformation behaviour of materials containing a fine dispersion of second phase particles. The particles influence the strength properties both directly and indirectly. They directly increase the matrix strength by slowing dislocation glide and climb and may also strengthen grain boundaries by interfering with grain boundary sliding and migration. Indirectly, the presence of the particles during the thermal-mechanical processing of the material may permit some control over the final microstructure. Thus the grain size and shape and possibly the dislocation substructure may be altered to increase the high temperature strength for a given alloy. Ideally these two effects should act together for the maximum benefit. For example, grain boundary sliding is an important mode of deformation at high temperatures. Thus the alignment of most of the grain boundaries parallel to the stress axis during thermo mechanical processing significantly reduces the contribution of grain boundary sliding to creep strain, thereby forcing deformation to occur within the grain where the direct strengthening mechanisms of the particles in the matrix can be used effectively.

An understanding of the mechanisms by which the particles directly influence the high temperature strength is still in the preliminary stages. Theories describing the interactions of particles with dislocations and grain boundaries at elevated temperatures have been formulated. However, with a few exceptions, a major difficulty has been the inability to isolate the various mechanisms experimentally, in order to quantitatively study the various particle effects. The exceptions have been the study of some aspects of particle-grain boundary interactions.

The influence of second phase particles on various aspects of the microstructure and on high temperature creep behaviour will be described. The theories describing creep mechanisms relating to dispersion strengthened systems will be discussed relative to their predictions concerning high temperature deformation behaviour and their relation to the observed properties.

Domanus: Methods of Fabrication and Measurement of Artificial Defects as Calibration Standards for Ultrasonic Inspection of Thin-walled Tubing (Risø Report No. 272 (1972) 24 pp.).

Information was collected on standards and reports of research work dealing with the problems of artificial defects for calibration of ultrasonic equipment used for the quality inspection of thin-walled tubes. Conclusions are drawn about the choice of the best method for producing and measuring artificial defects.

Domanus and N. Nielsen: Artificial Defects Used at Risø as Calibration Standards for Ultrasonic Inspection of Thin-walled Tubing (Risø Report No. 273 (1972) 24 pp.).

Artificial defects produced in zircaloy cladding tubes at Risø are described. They were used at the Danish Welding Institute for calibration of the ultrasonic equipment. The shape and dimensions of artificial defects were measured with the light section microscope, and after calibration measurements with the ultrasonic apparatus the test tubes were sectioned and the shape and dimensions of artificial defects were again measured with a metallographic microscope. The results of all those measurements are compared and evaluated.

Conclusions are drawn about the choice of the best method for producing and measuring artificial defects and about the necessity for further knowledge of the ultrasound field and shape of defects in order to establish a correct calibration procedure.

)omanus, A. Jensen, and B. S. Johansen: Assessment of the Homogeneity of Flat Reactor Fuel Plates by Densitometric Scanning of Radiographs (presented at the IVth National Scientific - Technical Conference on Non Destructive Testing, Varna, Bulgaria, June 1972. Not available).

Flat reactor fuel plates fabricated by the Elsinore Shipbuilding and Engineering Co., Ltd. for the Danish MTR reactor were examined by radiography. The radiographs were used for the assessment of uranium distribution in the fuel plates.

To determine the accuracy of the radiographic method, the X-ray films used were examined first. The quality of the radiation used for radiography was determined and characteristic curves of three X-ray film brands computed. Film speed and contrast were calculated. Film quality was evaluated by calculating standard deviations of film

densities in different exposure conditions. The source of error inherent in the X-ray film itself was determined.

Next, the correlation between film density and uranium content was established. For that purpose a calibration curve was plotted giving the relationship between the uranium content in the fuel plate and the equivalent aluminium thickness. From that curve the aluminium thickness was read corresponding to upper and lower tolerance limits in uranium content.

Fuel elements were assessed by comparing X-ray film densities under two aluminium strips with the above thicknesses placed together with the examined plate in a special cassette. Next radiographs of the plate (between Al-strips) were scanned on a densitometer (with paper chart recorder) and the plates were rejected if the densities on the X-ray films were beyond the tolerance limits.

The main difficulty was to calibrate X-ray films against plates with known uranium content. This was done by measuring doses of radiation under the plates with thermoluminescence dosimeters (produced at Risø) and comparing the results with calculations of uranium content (from weight and dimension measurements of the plates).

The described method can be used for assessment of the homogeneity of uranium content in flat reactor fuel plates for any given tolerance limits by establishing the aluminium thickness equivalent to those equivalent thicknesses.

G. Fayl and K. Hansen: In-Reactor Determination of the Thermal Conductivity of UO_2-Pellets up to 2200°C (Risø Report No. 269 (1972) 35 pp.).

The thermal conductivity of sintered stoichiometric UO_2-pellets was determined in the temperature range 500 -2200°C and at different burn-up levels from 0 to 0.8×10^{20} fiss/cm^3. The conductivity was evaluated from temperature measurements at the centre and two off-centre positions in the UO_2-pellets. The power was determined by thermocouples measuring temperature differences in the heat conduction path out from the UO_2-pellets. These thermocouples were power-calibrated by means of an electric furnace.

The rig design makes it possible to replace the centrally positioned thermocouple (during reactor shut-down) in the event of thermocouple failure or to eliminate irradiation-induced changes in its emf-characteristic. Furthermore, it is possible to replace the gases in the

fuel capsule in order to investigate the influence of fission gases on the fuel to cladding heat transfer.

The result of the experiment showed:

- Good agreement with literature data on thermal conductivity of UO_2 early in the irradiation (burn-up$\approx 10^{19}$ fiss/cm^3).
- A reduction in the thermal conductivity, with burn-up, at temperatures below 1000°C. This reduction caused a 9% increase of centre fuel temperature at a linear heat rating of 350 W/cm, after 0.8×10^{20} fiss/cm^3.
- No influence of burn-up on the thermal conductivity above 1000°C.
- No influence of fission gases on the fuel to cladding heat transfer (initial gap = 0.57% of fuel diameter).

With regard to the rig design, the system for exchange of the central thermocouple seems to be limited to a maximum fuel temperature of 1400°C.

H. E. Gundtoft and N. Nielsen: Fast and Accurate Non-destructive Testing Bench for Inspection of Canning Tubes (supporting paper at the Nuclex 72 exhibition, Basle, October 1972).

The development is described of an inspection bench for non-destructive examination of canning tubes. The bench is revolutionary in that the internal diameter is calculated from exact measurement of the outer diameter and the wall thickness. The transducers for inspection and control are rotated around the tube. Thus all measurements are made externally to the tube.

The results of these innovations is that non-destructive examination can be made in a single pass of the tube, and the assessment is more accurate, economical, and faster than that possible with existing technique.

N. Hansen: Superposition of Grain-Boundary Strengthening and Particle--Network Strengthening in Aluminium (Scripta Met. 5 (1971) 417-420).

Superposition of grain-boundary strengthening and particle-network strengthening has been studied in Al-Al_2O_3 products. It was found that a strength contribution from grain boundaries (σ_{gb}) can be added to the contribution from particle strengthening (σ_p). As a first approximation the following equation has been proposed for the flow stress

$$\sigma = \sigma_o + \sqrt{\sigma_{gb}^2 + \sigma_p^2} \ .$$

For the flow stress (0.2% offset) at room temperature and at 400°C, experimental results from 6 alloys support this equation with a reasonable accuracy.

N. Hansen: Room and Elevated Temperature Properties of Ball-Milled Aluminium - Aluminium Oxide Alloys (a Comment on a Paper by N. C. Kothari). J. Nucl. Mat. 43 (1 972) 339-340.

It is pointed out that the objective of Kothari's work, viz. the production of aluminium - aluminium oxide alloys with a uniform oxide distribution, is already fulfilled in commercial products. It is also shown that various conclusions drawn by Kothari are questionable.

N. Hansen: Recristallisation de produits renforcés par dispersion (Recrystallization of dispersion-strengthened materials) (presented at Journées Métallurgiques d'Automne, Chatenay-Malabry, France, October 1 972. Not available).

A general review is given of the effect of dispersed, hard particles on the recrystallization behaviour. It is observed that the recrystallization is retarded by a dense distribution of fine particles (interparticle spacings of 0.5 μm or less), whereas the recrystallization is accelerated when the interparticle spacing is 1 μm or more. The most important effect of the dispersed particles is probably their effect on the nucleation.

An experimental investigation of the recrystallization by isochronous annealing of dispersion-strengthened aluminium alloys is described. The alloys contained a distribution of fine aluminium-oxide particles with mean interparticle spacings of 0.2 - 0.5 μm. The effect of the particles was a retardation of the recrystallization. The retarding effect increased with decreasing particle spacing (for constant particle size) or with increasing particle size (for constant spacing). The retardation was also found to depend on the degree of cold work - it was less pronounced for the very high degrees. The interpretation of the results is discussed.

N. Hansen and B. Bay: The Effect of Particle Content, Particle Distribution and Cold Deformation on the Recrystallization of Low Oxide Al-Al_2O_3 Products (J. Mat. Sci. 7 (1972) 1351-1362).

The recrystallization of dispersion-strengthened Al-Al_2O_3 products containing 0.6 and 1.2 wt% Al_2O_3 was followed by optical and transmission electron microscopy and by hardness measurements. The recrystallization was retarded compared to aluminium and the important structural parameters were the oxide content (proportional to the reciprocal particle spacing) and the distribution of oxide particles either as a uniform distribution or as a regular three-dimensional network. From the microstructures after cold work and after recovery it is suggested that particle-retarded recrystallization may be caused by pinning, during the recovery stage, of sub-boundaries and of individual dislocations. The hypothesis of retardation of recrystallization as due to particle-enhanced homogenization of dislocation structures during deformation is not supported by the microstructural observations. In the product containing 0.6 wt% Al_2O_3 the recrystallization was markedly retarded after 50% cold reduction, whereas the retardation was small after 80 and 90% reduction. An increase in the degree of cold deformation may reduce the critical size of the recrystallization nuclei, and thus the retarding effect of particles during nucleation may be reduced or disappear. It is therefore suggested that the degree of cold deformation and the particle spacing may be interdependent parameters when determining the recrystallization behaviour of dispersion-strengthened products.

I. H. Qureshi, E. Larsen, L. Turi, J. Olsen, and H. Hougaard: Mass-spectrometric Measurement of Burn-up in UO_2 Fuel using Stable Fission-Product Neodymium (IAEA Symposium on Analytical Methods in the Nuclear Fuel Cycle, Vienna, November/December 1971. IAEA/SM-149/13 (1971)).

Among the stable fission products, neodymium has been proved to be a reliable burn-up monitor for various types of nuclear fuels. However, the chemical separation of neodymium from the irradiated fuel and other fission products is cumbersome and time consuming. Therefore a method has been developed for the mass-spectrometric determination of neodymium which does not require chemical separ-

ation of neodymium from the irradiated fuel. The fuel solution was spiked with enriched Nd-145, and the concentrations of Nd-143 and Nd-146 were determined by isotope-dilution mass-spectrometry. About 0.1 µg of neodymium is required to obtain an adequate ion current beam. Therefore for samples having low burn-up ($< 0.1\%$) it is necessary to use 3-4 mg of the fuel for mass-spectrometry. The maximum surface contact radiation dose of the samples varies from 200-400 mr/h. No interference from other nuclides was encountered in the measurement of Nd-143, Nd-145, and Nd-146. However, Ce-144, Pm-147 (Sm-147), Sm-148, and Sm-150 interfered in the measurement of Nd-144, Nd-147, Nd-148, and Nd-150 respectively. Therefore only Nd-143 and Nd-146 are used for calculating the burn-up. The reproducibility of the burn-up measurement with this method was checked by replicate analyses of control samples. Burn-up measurements were made on a number of irradiated UO_2 samples having burn--ups of 0.1 - 1.6%. The burn-up values obtained from Nd-143 and Nd-146 show about 2% variation between them.

The Nd-method is rapid and simple and can be used on a routine basis. The concentration of plutonium in UO_2 fuel can also be determined simultaneously by spiking the sample with Pu-242.

F. List and P. Knudsen: Pellet Stack Shortening and Cladding Elongation of Irradiated UO_2-Zr Fuel Pins (in: Aspects of Research at Risø. Risø Report No. 256 (1972) 45-52).

Six UO_2-Zr fuel pins irradiated to a burn-up of 5,600 MWD/te UO_2 showed pellet stack shortenings of 5 to 8 x 10^{-3} and pin elongations of 7 to 9 x 10^{-4}. A theoretical estimate, based on fuel - clad mechanical interaction and ratchetting, was made in an attempt to account for the length changes. The estimate for the pellet stack shortening agrees well with the observed values. The calculated pin elongation is lower than the measured values, probably because primary creep of Zr was neglected in the calculation.

T. Leffers: Theories for the Development of Deformation Textures (invited lecture held at the International Seminar on Quantitative Analysis of Textures, Krakow, Poland, September 1972. Not available).

By computer simulation it is demonstrated that both types of rolling texture observed in face-centred cubic materials can be produced by $\{111\}\langle 110\rangle$ slip. This makes assumptions of other deformation modes unnecessary. It is also shown that the most widely

accepted of the theories involving other deformation modes, the twinning theory, is not compatible with the author's experimental results. The transition from the brass-type to the copper-type texture is explained by cross-slip dispersion of the potential screw-dislocation pile-ups. The proposed model for the deformation of polycrystals and thus for the texture development, deviates from Taylor's ideas of homogeneous multiple glide - in agreement with the observed inhomogeneity of the deformation process.

R. M. J. Cotterill, T. Leffers and H. Lilholt: Molecular Dynamics Studies of Grain Boundaries (presented at the Microsymposium on Grain and Phase Boundaries in Metals, Gothenburg, Sweden, January 1972. Not available).

Grain boundaries in two-dimensional close-packed bicrystals are computer-generated. A liquid is brought to solidify between two slabs of crystal with the wanted angular misfit. The resulting grain boundaries are not straight, and their structure is more irregular than that suggested in the coincidence-boundary theories. The computer grain boundaries have a thin layer (few atomic diameters thick) with heavily distorted structure.

H. Lilholt: Comment on a Paper on Microstructural Parameters (presented at the conference on the Properties of Fibre Composites, Teddington, England, November 1971. Conference proceedings (IPC Science and Technology Press, Guildford, 1971) 14).

H. Lilholt: Review of Creep Theories for Fibre Composites (presented at the Third Nordic High Temperature Symposium, Risø, June 1972. Proceedings to be published).

Various models have been suggested as a description of the creep behaviour of fibre composites. They refer to composites with parallel fibres tested along the fibre direction, both long fibres and short fibres. The models consider loads carried by the fibres and by the matrix, and also the load exchange between fibres and matrix during a creep test. Rather few experiments have been made to test the models.

H. Lilholt: A Fibre Composite with Metallic Matrix for Use at High Temperatures - a Nordforsk Project (presented at the Third Nordic High Temperature Symposium, Risø, June 1972. Proceedings to be published).

Scandinavian Research Council (Nordforsk) is sponsoring a research project with participants from the Scandinavian countries. The aim is to establish experience within the field of fibre composites, to investigate the possibility of a composite with a metallic matrix for use above 800°C, and to make this new field known to the interested industry. The project involves methods for producing test specimens, the thermal stability including oxidation behaviour, and fatigue and creep properties.

J. Lindbo and T. Leffers: Preparing Dispersion-Hardened Materials for Transmission Electron Microscopy (Metallography 5 (1972) 473-477).

A new method for the preparation of thin foils of dispersion-hardened materials is described. The method has proved successful for materials with the following matrices: Aluminium, zirconium and zircaloy-2, ferritic iron, and stainless steel. The method also yields superb thin foils of the matrix materials without dispersoids.

P. D. Parsons and E. Adolph: Zirconium Alloys Dispersion-Strengthened with Yttria (Can. Met. Quart. 11 (1972) 223-235).

A powder metallurgy process for the manufacture of zirconium alloys dispersion-strengthened with yttria particles is described. The resulting alloys contain a suitable dispersion of stable yttria particles in a fine-grained matrix. Tensile and strength rupture tests over a range of temperature on zircaloy-2 containing 0, 5, and 10 vol% yttria show the strength of yttria-containing alloys to be significantly improved. The post-irradiation tensile properties of zircaloy-2-yttria alloys have been determined with alloys irradiated at 280°C to 9.2×10^{20} n/cm^2 thermal and 2.3×10^{20} n/cm^2 fast. The alloys have been subjected to accelerated corrosion tests in steam and exhibit a variable response. Some possible detrimental factors and means of improvement of properties are discussed.

The mechanical properties of zircaloy-2 alloys containing yttria particles are compared to some other zirconium alloys, zircaloy-2 and zirconium-2.5 wt% Nb, and the comparison shows that the dispersion-strengthened alloys are worthy of further development.

B. N. Singh: Simultaneous Reduction and Sintering of Mixed Oxides (J. Iron Steel Inst. 209 (1971) 306-307).

A method for producing stainless steels containing dispersions of stable oxide particles (almost completely free from chromic oxide) through the powder metallurgy route is suggested. Compacts of mixtures (with and without dispersions of alumina, zirconia, or titania) of ferric, nickel, and chromic oxides are first "fired" in air and subsequently reduced in a dry hydrogen atmosphere. The air "firing" stage of the process is thought to be very important for the complete reduction of the chromic oxide.

B. N. Singh: Pressure-Densification of Powder Composites (Powder Met. 14 (1971) 277-288).

A preliminary investigation of the pressure-densification behaviour of iron and nickel powders both with and without added alumina or zirconia particles has been made. The importance of some relevant parameters is assessed in the light of experimental results obtained on different powder composites, prepared by mechanical mixing of powders followed by compaction in a die using a hydraulic press.

The degree of pressure-densification decreases with increasing volume fraction of the added oxide particles, the decrease being also a function of the matrix and oxide particle-size ratio. These data are interpreted in terms of reductions in the number and area of the contact surfaces deforming as a result of the presence of non-deforming particles.

B. N. Singh: Compaction of Metal-Ceramic Powder Mixtures (in: Proceedings III Konferencji Metalurgi Prozkow, Zakopane, Poland, October 1971, 139-151).

The compaction behaviour of powder-composites containing "deforming" and "non-deforming" particles has been investigated. The importance of some relevant parameters is assessed in the light of experimental results obtained on different powder composites. The composites are prepared by mechanical mixing of iron or nickel and aluminium oxide or zirconium oxide powders followed by cold-compaction in a die using a hydraulic press.

The degree of pressure-densification decreases with increasing volume fraction of the added oxide particles, the decrease being also a function of the matrix/oxide particle-size ratio. The results are interpreted in terms of reduction in the number and area of the deforming contact surfaces arising due to the presence of the non-deforming particles. It is concluded that in a powder-composite of deforming and non-deforming particles, the latter has a substantial restrictive influence on its compaction behaviour.

B. N. Singh: Dissimilar-Surface Contacts and their Influence on Sintering Characteristics of Powder Composite Compacts (Powder Met. 15 (1972) 216-227).

In compacts containing metal and oxide particles, metal/oxide surface contacts modify the diffusional processes. Different distributions of such dissimilar-surface contacts and their influence on the sintering characteristics of some metal-oxide compacts are considered.

By selecting appropriate volume fractions and diameters of matrix and second-phase particles, structures containing different types of dissimilar surface contact distribution have been produced. Isochronal sintering of these structures clearly demonstrates that (a) the presence of chemically inert second-phase particles always hinders densification of the composite, (b) the sintering densification (for a given volume fraction of second-phase particles) is a strong function of (d_m/d_s), where d_m and d_s are the diameters of the matrix and second-phase particles, respectively, and (c) the nature of dissimilar-surface contact distribution has a significant effect on the densification of the composite.

O. Toft Sørensen: Thermogravimetric Studies of the High Temperature Thermodynamic Properties of Nonstoichiometric Cerium Oxides (presented at the Third International Conference on Thermal Analysis, Davos, Switzerland, August 1971. Proceedings (Birkhäuser, Basel, 1972) vol. 2, 31-42).

Thermogravimetric measurements of the oxygen dissociation pressure over nonstoichiometric cerium oxides have been carried out in the temperature range 900-1550°C in dynamic CO_2/CO atmospheres with oxygen pressures between 10^{-3}-10^{-22} atm corresponding to compositions in the range $1.98 > O/Ce > 1.73$. The oxygen pressure in the atmospheres used was accurately measured during the experi-

ments with a ZrO_2(CaO) solid electrolyte oxygen concentration cell. From the dissociation pressures measured, partial molar thermodynamic quantities for oxygen in the nonstoichiometric oxides are calculated and compared to low-temperature data previously reported. A detailed analysis of the free energy versus temperature plots shows that the oxygen-deficient fluorite CeO_{2-x} phase, which has previously been considered to be single phase above 650°C, apparently consists of several phases in the temperature range covered in the present experiments.

O. Toft Sørensen: Determination of Thermodynamic Properties of Oxides by High-Temperature Thermogravimetry (presented at the Nordforsk Symposium on Thermal Analysis, Helsinki, Finland, March 1972. Proceedings 97-107).

E. Tolksdorf and J. Lindbo: Electron Microscopical Investigation of the Metal-Oxide Interface of Zirconium Alloys (Praktische Metallographie 6 (1971) 371-374).

Ternary Zr-alloys with varying intermetallic particle size were subjected to oxidation in pure oxygen at 700°C, after which the interface between the metal and the oxide layer was investigated in the electron microscope. The investigation was centred on the migration of precipitated intermetallic particles.

D. Watson, M.R. Warren and C.J. Beevers: Some Observations of Ductile Void Growth and Crack Propagation in alpha-Zirconium (Can. Metal. Quart. 11 (1972) 53-59).

Tensile tests have been carried out on zirconium at 77°K to study the effects of unloading on ductile crack propagation and at 77°K, 295°K, and 423°K to examine the influence of matrix deformation characteristics on void growth rates. The effects of unloading are considered in terms of the relaxation at the crack tips, and estimates of the increased work necessary to propagate such relaxed cracks are consistent with the observed increases in fracture stress. The process of void growth was studied metallographically, and changes in void dimensions were measured as a function of specimen strain. These studies indicate that the strain increments at the void tips are most important in the void growth process, and that the void growth rate increases with increasing deformation temperature.

M. R. Warren and J. A. Ytterhus: Precipitation Reactions in Zr-2at%Cr-0.16at% Fe (Can. Metal. Quart. 11 (1972) 249-256).

The heat treatment which optimizes the corrosion resistance of Zr-2.0 at.% Cr - 0.16 at.% Fe is a β quench and age at 760°C. Rumball and Coleman have shown that if the quench rate is in the range 2000-7500°C/s, the subsequent ageing treatment leads to grain growth involving loss of strength and ductility. This work shows that the ageing in the temperature range 270-400°C induces precipitation prior to recrystallization, which may restrict grain growth at higher temperatures. The low-temperature precipitation is associated with two peaks in the resistivity isotherms, which become progressively less pronounced and occur at progressively shorter ageing times as the ageing temperature is raised. The precipitation process, involving the rejection of Cr and Fe from supersaturated solid solution, did not follow a simple rate law, but could be characterized by an activation energy of 0.93 ± 0.03 eV once equilibrium has been attained. Supplementary evidence shows that the resistivity peaks are probably associated with two distinct pre-precipitates which may be compared to the θ' precipitate found in Al-Cu alloys.

In Danish:

C. C. Agerup: Legeringslære (Alloys and Phase Diagrams) (Polyteknisk Forlag, Lyngby, 1972, 40 pp.).

The booklet gives an elementary introduction to the structure and properties of alloys, phase diagrams, annealing treatments, and phase transformations.

C. C. Agerup: Jern-Kulstofdiagrammet (the Iron-Carbon Phase Diagram) (Polyteknisk Forlag, Lyngby, 1972, 31 pp.).

The booklet gives an elementary introduction to the iron-carbon phase diagram and its relation to the structure and properties of iron and steel.

J. B. Bilde-Sørensen: Sekundær højtemperaturkrybning af polykrystallinsk magnesiumoxid (Secondary High-Temperature Creep of Polycrystalline Magnesium Oxide) (Risø-M-1385 (1971), thesis, 65 pp).

A review of the literature on the creep properties of ceramic materials is given. Also some of the models proposed for secondary high-temperature creep are discussed.

Experimentally the secondary creep of polycrystalline magnesium oxide with grain sizes of 100 and 190 μm has been examined at temperatures between 1300 and 1460°C and at compressive loads between 2.5 and 5.5 kp/mm^2. The dependence of creep rate upon load follows a power law with an exponent of 3.2. The process is thermally activated with an activation energy of 76 ± 12 kcal/mol. The creep rate is independent of grain size. The total dislocation density follows the relation $\sigma = bG\sqrt{\rho}$ that is commonly found for metals.

The dislocation structure is a three-dimensional network, which contains dislocations lying in their glide plane as well as dislocations lying in their climb plane. On the basis of this structure a model has been proposed where the main contribution to the deformation comes from glide, but where the rate-limiting process is diffusion-controlled. The agreement with the experimental results is within one order of magnitude.

J.B. Bilde-Sørensen: Specielle krybeprøvningsmetoder (Special Creep Test Methods) (Dansk Metallurgisk Selskabs Vintermøde, Lyngby, January 1972, Proceedings 99-107).

Advantages and disadvantages by creep test methods other than tensile creep testing are discussed. In particular compressive creep testing and tube creep testing are dealt with; the former as an example of a test chosen because of material properties, the latter as an example of test method choice based on the application of the material.

H. Carlsen: Trækprøvning af enkelte wolframfibre med tværsnitsdiameter i området 5-100 μm (Tensile Testing of Single Tungsten Fibres with Diameter in the Range 5-100 μm)(Dansk Metallurgisk Selskabs Vintermøde, Lyngby, January 1972, Proceedings 127-137).

Tensile testing of thin tungsten fibres to obtain values for Young's modulus, ultimate tensile strength, and elongation is described. In particular the handling difficulties such as the mounting of a thin fibre in a cardboard frame and the measurement of fibre diameter are dealt with. Differences in the results obtained from testing a single fibre and a bundle of fibres respectively, are briefly discussed.

J. Christensen: Moderne Loddeudstyr på Risø (Modern Equipment for Brazing and Soldering at Risø) (presented to the Dansk Svejseteknisk Landsforening, Copenhagen, November 1972. Not available).

J. Christensen: Lodning - Egenskaber og Processer (Brazing and Soldering - Properties and Processes) (three lectures presented to the Jydsk Svejseteknisk Forening, Jutland, November-December 1972. Not available).

N. Hansen: Dispersionshærdede materialer (Dispersion-Hardened Materials) (in: Beretning om Atomenergikommissionens Virksomhed i tiden 1. april 1970 til 31. marts 1971 (1971) 26-31).

A survey of the production and the properties of dispersion-hardened materials is given. Particularly dispersion-hardened aluminium, zirconium, and stainless steel are discussed.

N. Hansen: Økonomisk Materialevalg = Færre Omkostninger (Economical Selection of Materials = Reduced Costs) (Manegement 7 (1972) 166-168).

The selection of construction materials is described, and the organizational procedures for a correct selection are discussed. It is proposed that the materials information should be arranged in a schematic form.

B. S. Johansen: Elektronstrålesvejsning, Princip og Anvendelse (Electron Beam Welding, Principle and Application) (Dansk Teknisk Tidsskrift (1972) No. 7, 45-52).

The basic principle of electron beam welding is described, and some examples of typical industrial applications are given.

H. Lilholt: Mekaniske Egenskaber hos Fiberarmerede Metaller (Mechanical Properties of Fibre-reinforced Metals) (presented at the Fiberdag på den Kungliga Tekniske Högskolan, Stockholm, Sweden, May 1972).

A. Nielsen: Brudmekanisk prøvning (Fracture Mechanics Testing) (Dansk Metallurgisk Selskabs Vintermøde, Lyngby, January 1972, Proceedings 231-233).

The classical methods for control of steel quality do not provide any basis for evaluation of the probability of a catastrophic failure from a defect of a certain size in a structure of a certain steel loaded to a certain stress.

During the past decade mathematical analysis of the stress concentration at crack tips in elastic media of certain geometries have been successfully carried out. On the basis of this analysis special test pieces have been designed. From the information gained by the testing of a steel it is possible to calculate the relation between critical crack length causing fracture and the stress in a structure of that steel.

Some conditions, however, need to be fulfilled; one is that only a limited local plastic deformation takes place. That is the reason for the name of this method: Linear Elastic Fracture Mechanics (LEFM).

By far the largest amount of common steel structures produced to-day are made from tough steels developing large plastic zones at defects prior to fracture under loading. An approximation has been investigated on the basis of the Crack Opening Displacement (COD) which is the opening of an existing crack during loading up to the load causing the crack to propagate. The mathematical analysis is similar to the one used in LEFM.

A. Nielsen: Stålforskning (Research on the Safety of Steel Components) (in: Beretning om Atomenergikommissionens Virksomhed i tiden 1. april 1971 til 31. marts 1972 (1972) 27-38).

A general review is given of the present knowledge of the fracture mechanics of steel pressure vessels. The activities at Risø within this field and their background are described.

ORGANIZATION

(as at 31 December, 1972)

N. Hansen

A. M. Eichen
G. Olesen
G. Holm Lauritzen
M. Simonsen

Materials Testing and Development

E. Adolph

C. Bagger
K. Bryndum
H. Hougaard 5)
K. M. Laursen
A. Nielsen
B. Vigeholm

J. A. Aukdal
O. Eriksen
P. V. Jensen
J. Kjøller
B. Larsen
J. Larsen
B. Weiler Madsen
E. B. Mogensen
H. Nilsson
P. B. Olesen
T. R. Strauss

Physical Metallurgy

V. Andreasen 6)
J. Bilde-Sørensen 4)
H. Carlsen
A. Clauer 2)
P. O. Esbjørn 6)
T. Leffers
H. Lilholt
O. Bøcker Pedersen 6)
B. N. Singh
O. Toft Sørensen
M. R. Warren

H. Jensen
J. Lindbo
P. Nielsen

Materials Technology

H. E. Gundtoft

C. C. Agerup 3)
J. Christensen
J. Domanus 3)
A. Jensen 3)
B. S. Johansen
A. Lystrup
T. Green Nielsen 3)

I. Andersen
O. Chabert
K. E. Dysted Nielsen
H. Frederiksen
F. Jensen
K. E. Jensen
S. Langkilde Madsen
P. Dreves Nielsen
T. Nielsen
O. Olsen
J. Olsson

Project Group

P. Knudsen
J. Borring 3)
M. Kjær Petersen 3)
J. Stiff 1)

Corrosion

K. Rørbo

E. Tolksdorf

A. Rasmussen

Consultants

Gas analysis	S. Kühnel Hagen
Welding	E. Østgaard (Danish Welding Inst.)
Non-destructive Testing	N. Nielsen (Danish Welding Inst.)
Irradiation Damage	L. T. Chadderton (H. C. Ørsted Inst.)
Physical Metallurgy	R. M. J. Cotterill (Technical University of Denmark)

---

1) On leave of absence from the UKAEA
2) On leave of absence from the Batelle Memorial Institute, Colombo
3) On leave from the Elsinore Shipbuilding and Engineering Co., Ltd.
4) On leave of absence at the Department of Metallurgy, University of Oxford.
5) On leave of absence at the KFA, Jülich
6) Post-graduate student from the Technical University of Denmark